A Study of the Effects of Organic Modification and Processing Technique on the Luminescence Quenching Behavior of Sol−Gel Oxygen Sensors Based on a Ru(II) Complex

M. T. Murtagh* and M. R. Shahriari

Fiber Optic Materials Research Program, Rutgers—The State University, Piscataway, New Jersey 08854

M. Krihak

Nanogen, Inc., 10398 Pacific Center Court, San Diego, California 92121

Received April 14, 1998. Revised Manuscript Received September 2, 1998

The luminescence decay behavior of ruthenium(II)−tris-4,7-diphenyl-1,10-phenanthroline dichloride dissolved in different inorganic and organically modified silicate (ORMOSIL) sol−gel matrixes was investigated. Bulk xerogels and spin-coated thin films were synthesized from methyltrimethoxysilane (MTMS), tetraethyl orthosilicate (TEOS), and various molar ratios of the two precursors. Systematic changes in composition were conducted to examine the structural properties of sol−gel silicates for possible oxygen sensor supports. The luminescence behavior of the ruthenium complex quenched by oxygen was analyzed as a function of the sol−gel composition and processing technique. The Stern−Volmer ratio, indicative of the degree of luminescence quenching by oxygen, was found to increase with increasing additions of MTMS in the bulk xerogels. This improvement in oxygen sensitivity was attributed to the increased diffusivity in the less polar sol−gel matrix. Conversely, spin-coated thin films showed a decreasing Stern−Volmer ratio with increasing MTMS addition and, thus, a lower oxygen sensitivity than the inorganic TEOS samples. This contradictory quenching behavior was attributed to structural changes in the sol−gel matrix caused by the spin-coating process. In addition to luminescence decay measurements, XPS and ellipsometric studies were performed to evaluate the structural effects of MTMS on the properties of TEOS-derived xerogels and spin-coated thin films.

I. Introduction

For less than a decade, the immobilization of Ru(II) complexes in sol−gel hosts has been investigated for luminescence-based, fiber optic oxygen sensors.[1−5] Ruthenium complexes are an attractive class of compounds for luminescence oxygen-sensing applications, due to their high photochemical stability, high extinction coefficient, relatively long lifetime determined by the metal to ligand charge transfer (MLCT) excited states, large Stokes shift, and absorption spectra that nearly matches the emission spectrum of inexpensive, commercially available blue LED's.[6−10] As for the host material, sol−gel synthesis is a versatile technique in which the physical, chemical, and optical properties of the silicate-based gels are easily tailored.[11,12] These properties are modified by varying processing conditions such as the water to precursor ratio, solution pH, type of catalyst, and choice of precursor.[13−17] Among these parameters, the selection of precursor has provided significant changes in the quenching behavior of the guest Ru(II) molecules.[18,19]

Sol−gel derived silicates are synthesized by first hydrolyzing tetraethylorthosilicate (TEOS) in the pres-

(1) MacCraith, B. D.; McDonagh, C. M.; O'Keeffe, G. E.; Keyes, T.; Vos, J. G.; O'Kelly, B.; McGilp, J. F. *Analyst* **1993**, *118*, 385.
(2) MacCraith, B. D.; O'Keeffe, G.; McDonagh, C.; McEvoy, A. K. *Electron. Lett.* **1994**, *30*, 888.
(3) Shahriari, M. R.; Ding, J. Y.; Tong, J.; Sigel, G. H., Jr. *Proc. Soc. Photo-Opt. Instrum. Eng.* **1993**, *2068*, 224.
(4) Krihak, M.; Shahriari, M. R. *Electron. Lett.* **1996**, *27*, 12.
(5) Murtagh, M.; Ackley, D.; Shahriari, M. R. *Electron. Lett.* **1996**, *32*, 477.
(6) Bacon, J. R.; Demas, J. N. *Anal. Chem.* **1987**, *59*, 2780.
(7) Carraway, E. R.; Demas, J. N.; DeGraff, B. A.; Bacon, J. R. *Anal. Chem.* **1991**, *63*, 337.
(8) Li, X.-M.; Ruan, F.-C.; Ng, W.-Y.; Wong, K.-Y. *Sensors Actuators* **1994**, *B21*, 143.
(9) Demas, J. N.; DeGraff, B. A. *Anal. Chem.* **1991**, *63*, 829A.
(10) Li, X.-M.; Ruan, F.-C.; Wong, K.-Y. *Analyst* **1993**, *118*, 289.
(11) Hench, L. L.; West, J. K. *Chem. Rev.* **1990**, *90*, 33.
(12) Klein, L. C., Ed. *Sol−Gel technology for thin films, fibers, preforms electronics and specialty shapes*; Noyes: Park Ridge, NJ, 1988.
(13) Strawbridge, I.; Craievich, A. F.; James, P. F. *J. Non-Cryst. Solids* **1985**, *72*, 139.
(14) Buckley, A. M.; Greenblatt, M. *J. Non-Cryst. Solids* **1992**, *143*, 1.
(15) Ying, J. Y.; Benziger, J. B. *J. Non-Cryst. Solids* **1992**, *147*&*148*, 222.
(16) Pope, E. J. A.; Mackenzie, J. D. *J. Non-Cryst. Solids* **1986**, *87*, 185.
(17) Schmidt, H.; Scholze, H.; Kaiser, A. *J. Non-Cryst. Solids* **1984**, *63*, 1.
(18) McEvoy, A. K.; McDonagh, C. M.; MacCraith, B. D. *Analyst* **1996**, *121*, 785.
(19) Murtagh, M.; Krihak, M.; Ackley, D.; Shahriari, M. R. *J. Mater. Res.* In press.

10.1021/cm9802806 CCC: $15.00
Published on Web 11/04/1998

ence of an acid or base catalyst and then condensing the hydroxylated species to form an inorganic SiO_2 matrix. Applying sol−gel coatings to optical fibers has demonstrated promise in the area of oxygen gas sensors.[1−5] When these coatings are applied for dissolved oxygen (DO) measurements in aqueous solutions, however, it has been found that organically modified precursors improve the sensor's chemical durability, sensitivity, and dynamic range.[18,19] In these reports, methyltrimethoxysilane (MTMS) and methyltriethoxysilane (MTEOS) are the precursors of choice. Since these precursors contain three hydrolyzable alkoxy groups, the $Si-CH_3$ bond remains intact under typical sol−gel synthesis conditions. After gel formation, the nonbridging $Si-CH_3$ groups are part of the three-dimensional silicate backbone and structurally act as network modifiers that terminate the silicate network. Sol−gels formed from MTMS or MTEOS provide a less hydrophilic environment that is favorable for oxygen sensors, since oxygen permeation is generally greater in hydrophobic media.[20,21] Hence, the goal of utilizing an organically modified precursor such as MTMS is to provide the attractive hydrophobic characteristics while the favorable optical and thin film forming properties provided by sol−gel synthesis are maintained.

Due to the above-mentioned features of the sol−gel technique, sensor media derived from silicate precursors have been successfully demonstrated by monitoring the luminescence quenching of ruthenium(II)−tris-4,7-diphenyl-1,10-phenanthroline dichloride as a function of oxygen concentration.[1−5,18,19] The initial studies involving Ru(II) complexes immobilized in sol−gel matrixes illustrate the feasibility of applying these types of coatings for developing fiber optic oxygen gas and dissolved oxygen sensors. Even though sol−gel hosts show promise as an oxygen sensor transducer media, the interactions between the silicate host and Ru(II) complex molecules have not undergone the scrutiny that polymer matrixes have received.[22−26]

Optical sensors based on the luminescence quenching intensity or lifetime of a fluorophore are examined by Stern−Volmer analysis.[27] In homogeneous media with a single-exponential decay, the intensity and lifetime form of the Stern−Volmer equations with dynamic quenching are as follows:

$$I_0/I = \tau_0/\tau = 1 + K_{SV}[Q] \quad (1)$$

$$K_{SV} = k\tau_0 \quad (2)$$

where [Q] is the quencher concentration (i.e. partial pressure of oxygen), τ_0 is the lifetime in the absence of the quencher, τ is the lifetime in the presence of the quencher, and K_{SV} and k are the Stern−Volmer and bimolecular quenching constants, respectively. A single exponential describes the lifetime decay in homogeneous media and thus

$$D(t) = \alpha \exp(-t/\tau) \quad (3)$$

where $D(t)$ is the luminescence intensity at time t and α is the preexponential factor.

In heterogeneous media, however, eq 1 requires a modification to account for a nonlinear Stern−Volmer plot.[23,26] Since previous sol−gel reports have shown downward curvature in the Stern−Volmer interpretations, the following equation may be applied to describe a double-exponential approach:

$$I_0/I = 1/(f_{01}/(1 + K_{SV1}[Q]) + f_{02}/(1 + K_{SV2}[Q])) \quad (4)$$

where the f_{0i} variables are the fraction of the total emission from each component under unquenched conditions and the K_{SVi} variables are the associated Stern−Volmer quenching constants for each component. In this case, there are two lifetime components, and excited lifetime decay analysis may be described by

$$D(t) = \alpha_1 \exp(-t/\tau_1) + \alpha_2 \exp(-t/\tau_2) \quad (5)$$

where the subscripts 1 and 2 denote the assigned lifetime components.

For the description of dynamic quenching behavior, a pre-exponentially weighted mean lifetime (τ_m) has been reported by Demas et al.[30] that allows a direct comparison of lifetime and intensity data in microheterogeneous systems. The data are fitted to the sum of lifetimes and a τ_m is computed which is given by

$$\tau_m = \sum \alpha_i \tau_i / \sum \alpha_i \quad (6)$$

where α_i is the pre-exponential weighing factor associated with decay time τ_i. If only dynamic quenching is present, a modified Stern−Volmer equation using τ_{mo}/τ_m will match the intensity-based Stern−Volmer equation:

$$\tau_{mo}/\tau_m = I_0/I \quad (7)$$

In previous reports, sol−gel coatings are primarily prepared by dip-coating. Alternative sensor applications, however, may have a preference for spin-coated sol−gel films. By comparison, thin film formation by spin-coating undergoes a greater rate of solvent evaporation than by dip-coating or monolithic gel formation and, subsequently, changes the physical properties of the sol−gel.[29−32] To the best of our knowledge, luminescent, organic molecules have neither been applied as probes for investigating the local microenvironment of sol−gel spin-coated films nor has the luminescence quenching behavior of spin-coated films compared to

(20) Xu, W.; McDonough, R. C., III; Langsdorf, B.; Demas, J. N.; DeGraff, B. A. *Anal. Chem.* **1994**, *66*, 4133.
(21) Liu, H.-Y.; Switalski, S. C.; Coltrain, B. K.; Merkel, P. B. *Appl. Spectrosc.* **1992**, *46*, 1266.
(22) Bacon, J. R.; Demas, J. N. *Anal. Chem.* **1987**, *59*, 2780.
(23) Carraway, E. R.; Demas, J. N.; DeGraff, B. A.; Bacon, J. R. *Anal. Chem.* **1991**, *63*, 337.
(24) Draxler, S.; Lippitsch, M. E.; Klimant, I.; Kraus, H.; Woflbeis, O. S. *J. Phys. Chem.* **1995**, *99*, 3162.
(25) Li, X.-M.; Ruan, F.-C.; Ng, W.-Y.; Wong, K.-Y. *Sensors Actuators* **1994**, *B21*, 143.
(26) Hartmann, P.; Leiner, M. J. P.; Lippitsch, M. E. *Anal. Chem.* **1995**, *67*, 88.
(27) Lacowicz, J. R. *Principles of Fluorescence Spectroscopy*; Plenum Press: New York, 1983.
(28) Scriven, L. E. In *Better Ceramics through Chemistry III*; Brinker, C. J., Clark, D. E., Ulrich, D. R., Eds.; 1988; p 717.
(29) Brinker, C. J.; Hurd, A. J.; Schunk, P. R.; Frye, G. C.; Ashley, C. S. *J. Non-Cryst. Solids* **1992**, *147&148*, 424.
(30) Glaser, R. M.; Pantano, C. G. *J. Non-Cryst. Solids* **1984**, *63*, 209.
(31) Innocenzi, P.; Abdirashid, M. O.; Guglielmi, M. *J. Sol−Gel Sci. Technol.* **1994**, *3*, 47.
(32) Nakano, T.; Tokunaga, K.; Ohta, T. *J. Electrochem. Soc.* **1995**, *142*, 1303.

Table 1. Sol-Gel Compositions in Molar Ratios of Reagent:TEOS

gel designation	TEOS	MTMS	H_2O: precursor	EtOH	HCl
100% TEOS	1.0		2.0	2.5	0.0025
90% TEOS/10% MTMS	9.0	1.0	2.0	2.5	0.0025
80% TEOS/20% MTMS	4.0	1.0	2.0	2.5	0.0025
70% TEOS/30% MTMS	7.0	3.0	2.0	2.5	0.0025
60% TEOS/40% MTMS	3.0	2.0	2.0	2.5	0.0025
50% TEOS/50% MTMS	1.0	1.0	2.0	2.5	0.0025
40% TEOS/60% MTMS	2.0	3.0	2.0	2.5	0.0025
30% TEOS/70% MTMS	3.0	7.0	2.0	2.5	0.0025
20% TEOS/80% MTMS	1.0	4.0	2.0	2.5	0.0025
10% TEOS/90% MTMS	1.0	9.0	2.0	2.5	0.0025
100% MTMS		1.0	2.0	2.5	0.0025

bulk gels been directly investigated. Furthermore, despite the success of oxygen sensors prepared by sol−gel, little effort has been made to describe the nonlinear behavior of the Stern−Volmer curves. Consequently, the luminescence decay behavior of Ru(II) complexes in organically modified sol−gel matrixes has not been explored.

Thus, the goal of this paper is to provide insight on the luminescence decay of ruthenium(II)−tris-4,7-diphenyl-1,10-phenanthroline dichloride encapsulated in TEOS-based sol−gel compositions modified with MTMS. Also, the quenching behavior of Ru(II) molecules will be used to probe the effect of spin-coating these gel compositions. By comparing the luminescence decay behavior of the spin-coated films with that of the monolithic gels, conclusions will be drawn concerning the microstructural properties of the coatings as a function of organic modification. In addition, XPS, and ellipsometric analyses will be performed to further substantiate the conclusions derived from the luminescence experiments.

II. Experimental Section

II.1. Sol−Gel Preparation. *II.1.1. Bulk Gels.* The organically modified silicate (ORMOSIL) compositions are presented in Table 1. The organically modified precursor 98% methyltrimethoxysilane (MTMS), 99% tetraethyl orthosilicate (TEOS), and anhydrous ethyl alcohol were obtained from Aldrich. Concentrated HCl was purchased from Fisher Scientific. The organometallic complex ruthenium(II)−tris-4,7-diphenyl-1,10-phenanthroline dichloride was synthesized according to the procedure outlined by Watts and Crosby[33] and determined to be of high purity via HPLC. Typical absorption and emission spectra and the single exponential luminescence decay of Ru(II) dissolved in ethanol are shown in Figure 1. These constituents, including the Ru(II), were magnetically stirred continuously in a beaker for 15−18 h under ambient conditions (~25 °C). Gels were cast into polystyrene Petri dishes (2 in. diameter) with loosely capped lids. Samples were dried at 6 °C until bulk xerogels were formed. The drying time varied from 1 to 2 weeks for the gels with the gelation time decreasing for higher levels of MTMS. Bulk xerogels were approximately 0.02−0.1 mm thick. All gels were produced with a Ru(II) concentration of 1×10^{-5} M (moles of dye per liter of sol).

II.1.2. Coating Deposition. Sols were allowed to stand for ~1 h at room temperature (~25 °C) before deposition. Films were deposited on either circular 2 in. silicon substrates, 0.5 in. silica glass disks (Esco, Inc.), or silica cover glass slips (Corning, Inc., Product #2875). Substrates were cleaned by first etching in a 1 N HF solution (Fisher Scientific) for 60−90 s and then spinning the following series of solutions onto the substrates for 30 s: anhydrous methanol (Fisher Scientific) and deionized water. The solution spinning was repeated three times to thoroughly clean the substrate. A commercial spin-coater (Specialty Coating Systems, Inc., Model #P6204) was used to deposit spin-coated films onto the various substrates. After depositing enough sol to cover the entire substrate, it was spun for 30 s at a frequency of 3000 rpm. The silicon wafers were used as substrates for ellipsometric measurements while the sol−gel coated silica disks and cover slips were used for both film characterization and lifetime measurements.

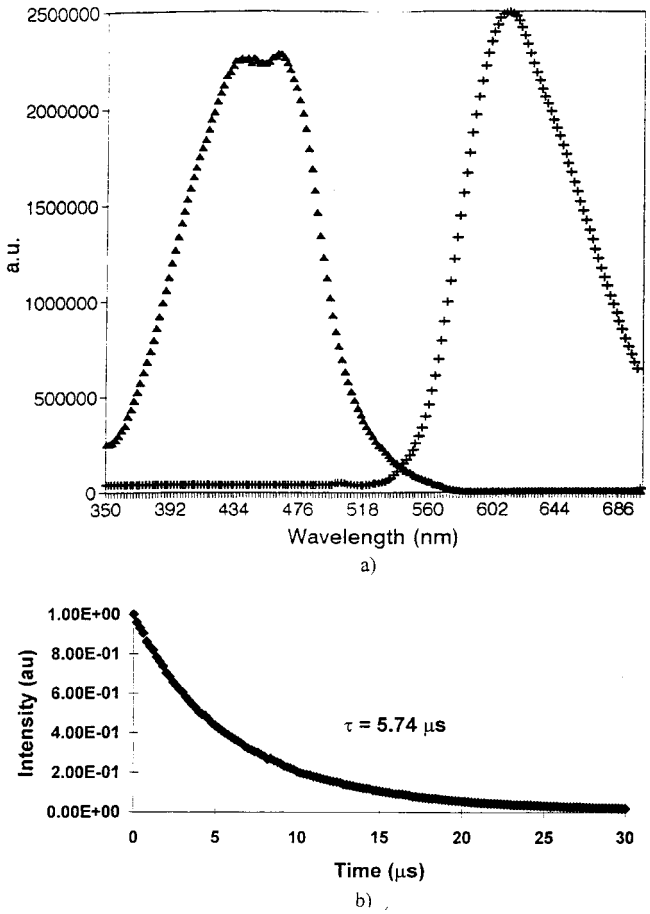

Figure 1. (a) Absorption and emission spectra of Ru(II) in solution (1×10^{-5} M); (b) Excited-state decay curve for Ru(II) in solution under unquenched conditions.

II.2. Lifetime Measurement. A pulsed nitrogen dye laser (Laser Science, Inc.) was used as the excitation source (excitation $\lambda_{max} = 450$ nm) and a fast photomultiplier tube (Hamamatsu, Inc., Model R928) as the detector (rise time = 2 ns). Each sample was exposed to 2 ns laser pulses (laser power = 1 mW, irradiation area of excitation pulse ~2 mm) until equilibration was reached at each oxygen concentration level. This equilibration time varied from seconds for the thin films to tens of minutes for the bulk gels (exact time depended on the sample composition). Due to interference from the excitation source, geometrical considerations resulted in a sample orientation of 90°, to remove reflected and scattered excitation from entering the detector. The luminescence emission was monitored through a 600 nm cutoff filter (Newport, Inc) to eliminate stray room and pump light. The signal from the PMT was relayed through a 50 Ω termination plug that was passed into a digitizing oscilloscope (Hewlett-Packard 54520A) that was used to resolve the lifetime decay curves. All measured lifetimes presented were averaged between 600 and 2400 times. Electronic mass flow regulators (Tylan General) were used to control the flow of nitrogen, dry air (~22% oxygen), and oxygen into the closed sample chamber. Measurements were taken continuously until equilibrium was reached in the

(33) Watts, R. J.; Crosby, G. A. *J. Am. Chem. Soc.* **1971**, *93*, 3184.

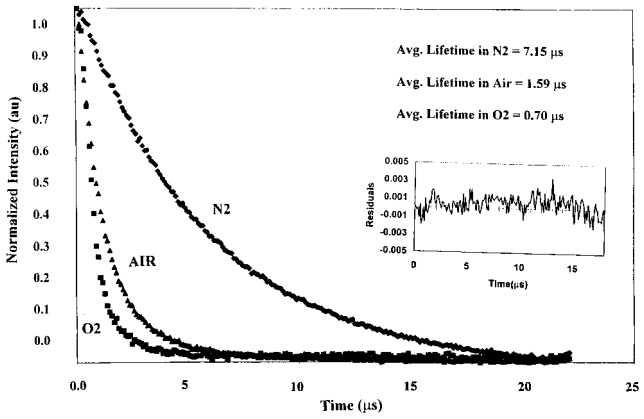

Figure 2. Excited-state decay curves for a 100% MTMS bulk xerogel sample doped with the Ru complex (1×10^{-5} M); inset, residual plot.

chamber, and decay curves were fitted by a least-squares algorithm using various commercially available software packages. All measurements were performed at ~25 °C.

II.3. Analytical Techniques. *II.3.1. XPS.* Surface spectroscopy was performed (Model XSAM 800, Kratos Analytical, Ramsey, NJ) using a sample exposure and preparation chamber with XPS capability. This system was equipped with a Mg Kα X-ray (1253.6 eV) source, and the base pressure of the spectrometer chamber was 2×10^{-9} Torr. The electron spectrometer was calibrated by assuming the binding energy of the gold $4f_{7/2}$ line at 83.9 eV with respect to the Fermi level. Samples were analyzed at a polar angle of 60° between the normal to the sample surface and the detector axis. This geometry permits the detection of photoelectrons escaping from a depth within the range of 1.5−2.5 nm.

II.3.2. Ellipsometry. Refractive index and thickness of spin-coated films were determined by the Rudolph Auto/EL ellipsometer. The properties of the gel samples were characterized at a wavelength of 632.8 nm. Compositions of 100% MTMS, 50% MTMS/50% TEOS, and 100% TEOS were examined at room temperature under ambient conditions (~25 °C). Porosities were calculated from the refractive indices via the Lorentz−Lorentz relationship, which is defined as

$$(n_f^2 - 1)/(n_f^2 + 2) = V_s(n_s^2 - 1)/(n_s^2 + 2) \qquad (8)$$

where n_f is the refractive index of the film, n_s is the refractive index of the solid skeleton, and V_s is the volume fraction solids. The refractive index of the solid silica skeleton was assumed to be 1.458. All data given represent averages of 10 points.

Results

III.1. Lifetime Analysis. *III.1.1. Bulk Xerogels.* Some examples of the quenching effects of oxygen on the fluorescence lifetime of Ru(II) are shown in Figures 2 and 3 for the 100% MTMS and 100% TEOS xerogels, respectively. Decay curves are best described by a double exponential model. Figures 4 and 5 show intensity and lifetime Stern−Volmer quenching plots for various xerogels ranging from 100% MTMS to 100% TEOS. Downward curvature is exhibited in all plots and is indicative of heterogeneous quenching, as previously observed by Demas et al.[20,22−23] and others[24,26,34] in various polymers. Intensity and lifetime measurements provided similar Stern−Volmer curves, revealing an exclusively dynamic quenching process.[23] Values of

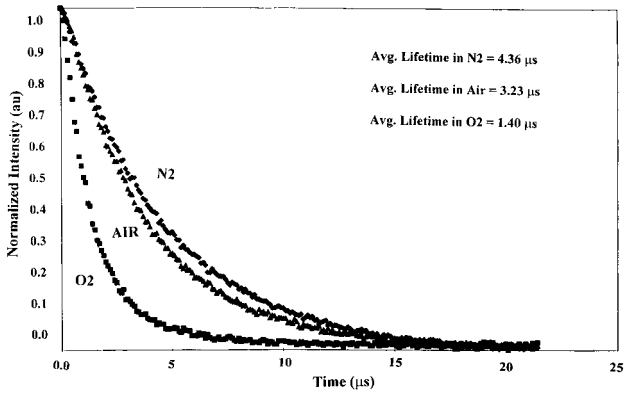

Figure 3. Excited-state decay curves for a 100% TEOS bulk xerogel sample doped with the Ru complex (1×10^{-5} M).

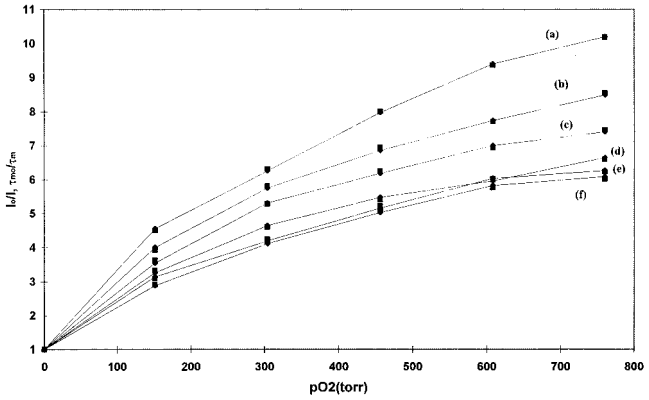

Figure 4. Stern−Volmer plots of Ru-doped xerogels: (a) 100% MTMS; (b) 90% MTMS/10% TEOS; (c) 80% MTMS/20% TEOS; (d) 70% MTMS/30% TEOS; (e) 60% MTMS/40% TEOS; (f) 50% MTMS/50% TEOS) [diamonds = lifetime data; squares = intensity data].

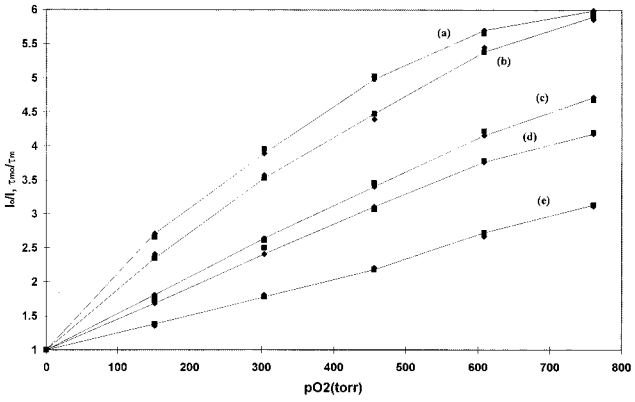

Figure 5. Stern−Volmer plots for Ru-doped xerogels: (a) 40% MTMS/60% TEOS; (b) 30% MTMS/70% TEOS; (c) 20% MTMS/80% TEOS; (d) 10% MTMS/90% TEOS; (e) 100% MTMS) [diamonds = lifetime data; squares = intensity data].

the intensity-based Stern−Volmer quenching constants (K_{SV}) are listed in Table 2. In the MTMS-modified xerogels, there is a distinct difference in the K_{SV} values for each sample. This result is indicative of site heterogeneity in which one site is more heavily quenched than the other.[24,26] For the inorganic TEOS gel, however, the K_{SV} values are almost identical and yield a nearly linear I_0/I vs p_{O_2} plot. This result suggests that the TEOS xerogel provides a host with greater site homogeneity than the MTMS-derived xerogel. A final trend in the data reveals that the more heavily weighted

(34) Demas, J. N.; DeGraff, B. A.; Xu, W. *Anal. Chem.* **1995**, *67*, 1377.

Table 2. Intensity-Based Stern−Volmer Quenching Constants for Ru(II)-Doped Xerogels

composition	I_0/I_{oxygen}	K_{sv1}	K_{sv2}	f_{01}	f_{02}
100%TEOS	3.11	0.0029	0.0029	0.96	0.04
90% TEOS/10% MTMS	4.17	0.0047	0.0012	0.97	0.03
80% TEOS/20% MTMS	4.67	0.0055	0.0013	0.95	0.05
70% TEOS/30% MTMS	5.90	0.0093	0.0006	0.96	0.04
60% TEOS/40% MTMS	5.94	0.0121	0.0007	0.95	0.05
50% TEOS/50% MTMS	6.07	0.0146	0.0004	0.92	0.08
40% TEOS/60% MTMS	6.22	0.0170	0.0002	0.92	0.08
30% TEOS/70% MTMS	6.58	0.0268	0.0002	0.87	0.13
20% TEOS/80% MTMS	7.44	0.0252	0.0001	0.92	0.08
10% TEOS/90% MTMS	8.54	0.0295	0.0001	0.92	0.08
100%MTMS	10.17	0.0360	0.0003	0.92	0.08

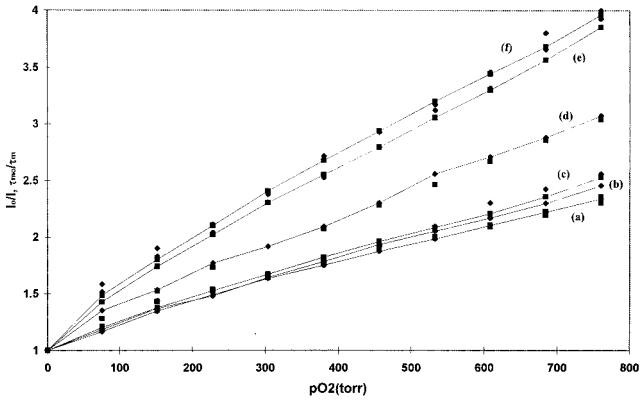

Figure 6. Stern−Volmer plots for Ru-doped spin-coated samples: (a) 100% MTMS; (b) 90% MTMS/10% TEOS; (c) 80% MTMS/20% TEOS; (d) 70% MTMS/30% TEOS; (e) 60% MTMS/40% TEOS; (f) 50% MTMS/50% TEOS) [diamonds = lifetime data; squares = intensity data].

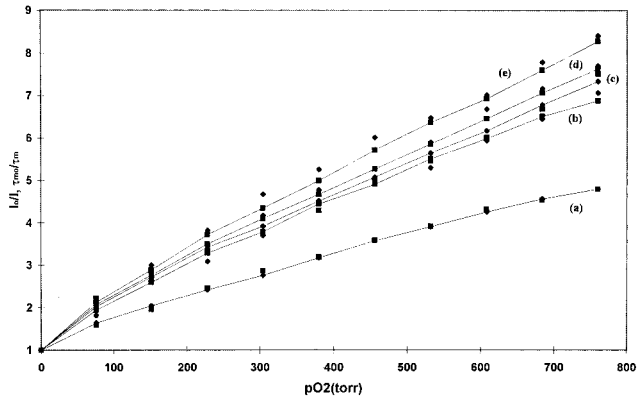

Figure 7. Stern−Volmer plots for Ru-doped spin-coated samples: (a) 40% MTMS/60% TEOS; (b) 30% MTMS/70% TEOS; (c) 20% MTMS/80% TEOS; (d) 10% MTMS/90% TEOS; (e) 100% TEOS) [diamonds = lifetime data; squares = intensity data].

K_{SV1} value for the individual gel samples increases with greater concentrations of MTMS.

III.1.2. Spin-Coated Thin Films. Stern−Volmer intensity and lifetime plots are represented in Figures 6 and 7 for an entire range of organically modified, spin-coated sol−gel samples. Examination of the oxygen partial pressures up to 1 atm reveals a downward curvature of these plots, indicating heterogeneous quenching. All decay curves are best described by a double-exponential model. Matching intensity and lifetime Stern−Volmer quenching plots are evident, which is representative of an exclusively dynamic quenching process.[23]

Table 3. Intensity-Based Stern−Volmer Quenching Constants for Ru(II)-Doped Spin-Coated Thin Films

composition	I_0/I_{oxygen}	K_{sv1}	K_{sv2}	f_{01}	f_{02}
100% TEOS	8.40	0.0266	0.0031	0.70	0.30
90% TEOS/10% MTMS	7.69	0.0312	0.0033	0.63	0.37
80% TEOS/20% MTMS	7.50	0.0318	0.0032	0.61	0.39
70% TEOS/30% MTMS	7.05	0.0150	0.0013	0.84	0.16
60% TEOS/40% MTMS	4.78	0.0123	0.0017	0.67	0.33
50% TEOS/50% MTMS	4.00	0.0148	0.0019	0.52	0.48
40% TEOS/60% MTMS	3.93	0.0220	0.0024	0.32	0.68
30% TEOS/70% MTMS	3.07	0.0173	0.0019	0.22	0.78
20% TEOS/80% MTMS	2.56	0.0108	0.0014	0.21	0.79
10% TEOS/90% MTMS	2.35	0.0065	0.0012	0.30	0.70
100% MTMS	2.30	0.0044	0.0007	0.54	0.46

A two-site model is suffice to fit the intensity quenching data of the Ru(II)-doped thin films. Intensity-based Stern−Volmer quenching constant (K_{sv}) data are listed in Table 3 for the spin-coated samples. The analysis provides quenching constants, $K_{sv1}{}^i$ and $K_{sv2}{}^i$, differing by a factor of ∼10. The fractional contributions of the components are also listed in Table 3. In comparison to the xerogel samples, the spin-coated films have greater contributions from the weaker contributing K_{SV} value.

Note the quenching behavior of the 100% TEOS spin-coated thin film doped with Ru(II) as compared with the MTMS-modified samples. According to the Stern−Volmer quenching plots presented in Figures 6 and 7, the Stern−Volmer ratio, τ_{N_2}/τ_{O_2}, is determined to be 8.4 for the inorganic, TEOS-derived sample. As the MTMS content is gradually increased, the Stern−Volmer ratio is found to decrease. In fact, this ratio drops to 4.0 and 2.3 for the 50% MTMS/50% TEOS and 100% MTMS spin-coatings, respectively. This decrease in the luminescence quenching of the organically modified films represents a reduction in the oxygen sensitivity over the TEOS-derived coating. These results are contradictory to those discussed in the previous section for bulk gels. In shifting from the TEOS to MTMS spin-coated samples, the sensitivity drops by a factor of 4. Contradictory to the spin-coating results, xerogels derived from TEOS are a factor of 3 less sensitive than the MTMS-derived xerogels. Even though similar sol−gel solutions are utilized, it may be concluded that the method of gel formation plays an important role in the behavior of the oxygen transducer.

III.2. Structural Analysis. *III.2.1. XPS. III.2.1.1 Bulk Gels.* Table 3 lists XPS data for the C 1s-, O 1s-, and Si 2p-photoelectron lines in 100% TEOS, 50% MTMS/50% TEOS, and 100% MTMS bulk gels. A primary feature of the table is a summary of the atomic concentration of carbon at the surfaces of the gels. The atomic concentration of carbon at the gel surface of 100% MTMS is 50.29%, as compared to 38.91% for the 50% MTMS/50% TEOS gel and 23.38% for the 100% TEOS gel. The higher concentration of carbon in the 100% MTMS sample is mostly due to nonhydrolyzable methyl groups ($Si-CH_3$) and partly to residual, unreacted −OR groups. The higher carbon concentration in the organically modified bulk samples thus represents an increase in the surface hydrophobicity over the inorganic TEOS gel. In the 100% TEOS sample, a carbon concentration of 23.38% is a high value for an inorganic gel. However, this result is plausible since a substoichiometric amount of water was used in the gel

Table 4. XPS Data for Sol−Gel Bulk and Thin Film Samples

composition	element	atomic concentration (%) bulk	spin-coated
MTMS	C	50.29	31.87
	O	32.73	43.28
	Si	16.98	24.85
50% TEOS/50% MTMS	C	38.91	26.96
	O	41.11	49.60
	Si	19.99	23.43
TEOS	C	23.38	25.43
	O	53.84	53.97
	Si	22.78	20.60

process and the gels were dried at low temperature (∼50 °C). Accordingly, this allows only partial hydrolysis to occur, and consequently, a gel results with many residual, unreacted Si−OR groups still present. Furthermore, heating at low temperature does not induce these Si−OR groups to hydrolyze. These residual Si−OR groups have been observed by FTIR in low temperature-heated sol−gel materials in previous investigations.[35−38]

III.2.1.2. Spin-Coated Thin Films. Table 4 lists XPS data of the O 1s-, C 1s-, and Si 2p-photoelectron lines for 100% TEOS, 50% MTMS/50% TEOS, and 100% MTMS spin-coated thin film. The atomic surface concentrations of oxygen and carbon are similar for the 100% TEOS thin film as compared to the bulk gel. The carbon content appears to be primarily attributed to residual OR groups, as previously observed in XPS and Auger analyses on acid-catalyzed TEOS spin-coated thin films by Brow and Pantano.[39−41]

In contrast to the bulk xerogels, however, organically modified spin-coated thin films consist of different carbon and oxygen concentrations. In the 100% MTMS thin film, the surface carbon concentration decreases from 50.29% in the xerogel to 31.87% in the spin-coated material. The surface oxygen concentration increases from 32.73% to 43.28% with respect to the MTMS bulk samples. It may be inferred from these results that a greater concentration of $Si-CH_3$ moieties resides below the gel surface in the spin-coated films. Accordingly, a greater oxygen concentration indicates a less hydrophobic surface for the organically modified spin-coated thin-films. The TEOS-based xerogel and spin-coated film, however, possess similar atomic concentrations. This result suggests that the chemical constituents at the gel surface, by either preparation method, are the same. Hence, the difference in oxygen-quenching behavior is due to the gel microstructure/morphology.

III.2.2. Ellipsometry. Table 5 lists refractive index, film thickness, and porosity results for the 100% TEOS and organically modified spin-coated films. The refractive index was determined to be 1.44 for the 100% MTMS sample, 1.41 for the 50% MTMS/50% TEOS sample, and 1.36 for the inorganic 100% TEOS thin film. Porosities were calculated from the refractive indices via the Lorentz−Lorentz relationship. The increase in refractive index with MTMS modification is indicative of a lower porosity in the organically modified samples. Consequently, the porosity was determined to decrease from 19.1% for the 100% TEOS thin film to 3.4% for the 100% MTMS sample.

Table 5. Ellipsometry Results for Spin-Coated Samples[a]

sample	film thickness (nm)	SD	refractive index	SD	calcd porosity (%)
100% MTMS	110	2.1	1.44	0.023	3.41
50% TEOS/50% MTMS	170	2.5	1.41	0.019	9.20
100% TEOS	90	2.6	1.36	0.018	19.12

[a] Spin rate = 3000 rpm. All results are 10-point averages. Porosities are calculated via the Lorentz−Lorentz relationship. SD = standard deviation.

IV. Discussion

IV.1. Effect of Organic Modification by MTMS. *IV.1.1. Bulk Gels.* From the Stern−Volmer calibration curves and the K_{SV} values, it may be concluded that the MTMS precursor enhances the heterogeneous quenching and nonlinear Stern−Volmer plot in the TEOS-based xerogels. This tendency toward heterogeneous quenching may be attributed to the structural and chemical influences of using MTMS as a sol−gel precursor, due to the lack of sites in MTMS-modified gels as compared to a TEOS gel.[31,38,42−45] Since MTMS has three alkoxy groups that undergo hydrolysis (whereas TEOS has four), only three linkages may form bridging oxygen bonds that contribute in the development of the silicate network. The fourth alkyl species is a nonhydrolyzing methyl group that is inert throughout the hydrolysis and condensation reactions and acts as a network terminator. Hence, the silicate network has terminating groups in the form of the organic $Si-CH_3$ species and yields a more open structure than the TEOS gel.[42−44] Besides providing structural modification, a second influence of MTMS is the introduction of an organic group into the sol−gel network. Chemically, the $Si-CH_3$ group in the dried gel is nonpolar and is thermally stable up to 400 °C.[31,44] As a result, introduction of the organic functional groups into the silicate structure may create regions within the gel matrix which are highly nonpolar. Consequently, these microheterogeneities may result in lifetimes that exhibit double exponential decay behavior in the presence of oxygen.

By relating this argument to the Stern−Volmer calibration curves and the K_{SV} values, it may be inferred from the data that the heterogeneous quenching is a result of oxygen permeation into two types of sites within the sol−gel matrix where each site is described by a specific K_{SV} (or lifetime) value.[20,23] In this case, the

(35) Brinker, C. J.; Scherer, G. W. *Sol−Gel Science*; Academic Press: New York, 1990.
(36) Orcel, G.; Phalippou, J.; Hench, L. L. *J. Non-Cryst. Solids* **1986**, *88*, 114.
(37) Yoshino, H.; Kamiya, K.; Nasu, H. *J. Non-Cryst. Solids* **1990**, *126*, 68.
(38) Krihak, M.; Shahriari, M. R. *Optical Mater.* **1996**, *5*, 301.
(39) Pantano, C. G.; Brow, R. K.; Carman, L. A. in *Sol−Gel Technology for Thin Films, Fibers, Preforms, Electronics, and Specialty Shapes*; Klein, L. C., Ed., Noyes: Park Ridge, NJ, 1988; Chapter 6.
(40) Brow, R. K.; Pantano, C. G. *J. Am. Ceram. Soc.* **1987**, *70*, 9.
(41) Pantano, C. G.; Glaser, P. M.; Armbrust, D. J. In *Ultrastructure Processing of Ceramics, Glasses, and Composites*; Hench, L. L., Ulrich, D. R., Eds.; Wiley: New York, 1984; Chapter 13.
(42) Li, X.; King, T. A. *J. Non-Cryst. Solids* **1996**, *204*, 235.
(43) DeWitte, B. M.; Commers, D.; Uytterhoeven, J. B. *J. Non-Cryst. Solids* **1996**, *202*, 35.
(44) Kamiya, K.; Yoko, T.; Tanaka, K.; Takeuchi, M. *J. Non-Cryst. Solids* **1990**, *121*, 182.
(45) van Bommel, M. J.; Bernards, T. N. M.; Boonstra, A. H. *J. Non-Cryst. Solids* **1991**, *128*, 231.

lower K_{SV} value (related to a longer lifetime value) corresponds to the series of sites which are not easily quenched by oxygen. Therefore, these sites are more likely characterized by lower diffusion rates that inhibit luminescence quenching by oxygen in these regions. Conversely, a second series of sites also exists that is more accessible to oxygen, which is indicated by the higher K_{SV} value (related to a shorter lifetime value). In the MTMS-modified gels, the double exponential is always represented in the presence of oxygen. On the other hand, the TEOS gel shows less tendency toward double exponential decay, even in the presence of higher oxygen partial pressures. This may indicate fewer microheterogeneities in these gels and, thus, less heterogeneous (or more homogeneous) quenching. This point is further evidenced by the almost linear Stern−Volmer plot for the 100% TEOS sample.

According to Figures 4 and 5, the Stern−Volmer ratios, τ_{N_2}/τ_{O_2} and τ_{N_2}/τ_{AIR}, are found to be greater in the MTMS-modified gels. This result is attributed to the decreased polarity provided by the nonhydrolyzing Si−CH_3 functional group. It has been reported previously by Demas et al.[23] that the Ru(II) complex is subject to improved luminescence quenching by oxygen when immobilized in materials of increased nonpolarity. According to their work, polymers of greater nonpolarity are more permeable to oxygen. In addition, it has been shown by Innocenzi et al.[31] and Matsui et al.[48] that the number of surface Si−CH_3 groups increases with increasing ratio of ORMOSIL (MTMS, MTES, etc.) to TEOS. The Si−CH_3 groups replace the surface Si−OH groups, thereby enhancing the surface hydrophobicity. An analogous point is in the recent work of Reetz et al.,[49] in which it was shown that the entrapment of lipases in sol−gel is dramatically improved by the use of hydrophobic silane precursors (such as MTMS, MTES, etc.), which lead to a phase separation from the surrounding aqueous phase during the condensation process. Similarly, the XPS analysis in this report provides strong support for MTMS-modified xerogels providing a more suitable host for oxygen-sensing applications than TEOS. The greater surface carbon concentration in the organically modified bulk samples, due to Si−CH_3 moieties, represents an increase in the surface hydrophobicity over the inorganic TEOS xerogel. Moreover, the addition of MTMS to the TEOS-derived xerogels increases the contribution of the more highly quenched, short-lifetime component in the presence of oxygen and raises the Stern−Volmer ratio. Therefore, the MTMS precursor improves the sensitivity of the xerogels toward lower oxygen concentrations due to the increased oxygen diffusivity (or permeability) in these more hydrophobic gels.

Inspection of the Stern−Volmer quenching curves (Figures 4 and 5), in conjunction with Figures 2 and 3 (decay profiles), provides additional evidence that the MTMS-modified gels are more sensitive to lower levels of oxygen than TEOS-derived gels. By comparing the decay profiles (Figures 2 and 3), the TEOS-derived sample in dry air (approximately 22% oxygen) shows a luminescence decay behavior with a slope that is less than that of the unquenched sample. Not until the gel is exposed to pure oxygen does the TEOS sample undergo a large change from the initial, unquenched decay profile. However, the Ru(II) complex entrapped in the MTMS sample experiences greater quenching by oxygen when exposed to air than the TEOS sample. This dramatic change in the luminescence decay behavior from nitrogen to air is followed, qualitatively, by a smaller change when exposed to oxygen.

Overall, the combination of the chemical and physical effects, provided by the MTMS precursor, has improved the Stern−Volmer quenching ratio of the Ru complex in the bulk samples. Besides improving the degree of quenching, MTMS is thus found to induce a xerogel that is more sensitive to oxygen at lower concentrations than one derived from TEOS. In previous studies, sol−gel oxygen sensors based on MTMS were shown to be extremely sensitive at low oxygen concentrations.[4−5,19,46−47]

IV.1.2. Spin-Coated Thin Films. Glaser and Pantano[30] determined that increasing the water/TEOS ratio increases the density of the TEOS spin-coated thin films, in contrast to the situation observed in bulk gels. This difference was rationalized on the basis of microstructure. The gels produced from solutions of high water content undergo enhanced hydrolysis, and therefore, more highly condensed species are formed. In the bulk case, the gelation occurs slowly and in the presence of an organic solvent phase. The polymerizing oxide phase forms spherical particles, and thus, a coarse, low-density gel results due to the poor packing of these particles.

In contrast, a spin-coated film structure undergoes polymerization simultaneous with, or consequential to, the evaporation of the organic solvent phase. Under these conditions, the formation of coarse spherical particles is unlikely. Instead, there will be an enhanced polycondensation within the plane of the film. Thus, solutions of increasing water/TEOS ratio yield dried gel films of greater initial density.[30]

Since the TEOS spin-coated thin films used in the present study are synthesized with a low water/TEOS ratio, a thin film of low density is expected. This result is observed by the low refractive index (hence, greater porosity) measured by ellipsometry. The increased porosity in the TEOS spin-coated thin film improves the accessibility of oxygen to the Ru(II) molecules encapsulated in the film. Thus, a greater Stern−Volmer ratio and enhanced oxygen sensitivity over the bulk TEOS gels is recognized for TEOS-derived spin-coated films.

On the other hand, the organically modified thin films are more dense, or less porous, than the TEOS films and the MTMS xerogels. This result may be attributed to the greater flexibility (compliancy) of methyl groups in the MTMS-modified films.[31] MTMS-derived gels are believed to form linear-type polymeric chains,[44] which upon spinning, may compact the gel structure as the chains become preferentially aligned and stack under the centrifugal conditions. The structure of TEOS, however, is that of a rigid, three-dimensional oligomeric

(46) Krihak, M.; Shahriari, M. R. *Proc. Soc. Photo-Opt. Instrum. Eng.* **1995**, *2508*, 358.
(47) Murtagh, M. T.; Krihak, M.; Kwon, H. C.; Shahriari, M. R. *Proc. Soc. Photo-Opt. Instrum. Eng.* **1996**, *2836*, 87.
(48) Matsui, K.; Tominaga, M.; Arai, Y.; Satoh, H.; Kyoto, M. *J. Non-Cryst. Solids* **1994**, *169*, 295.
(49) Reetz, M. T.; Zonta, A.; Simpelkamp, J.; Rufinska, A.; Tesche, B. *J. Sol−Gel Sci. Technol.* **1996**, *7*, 35.

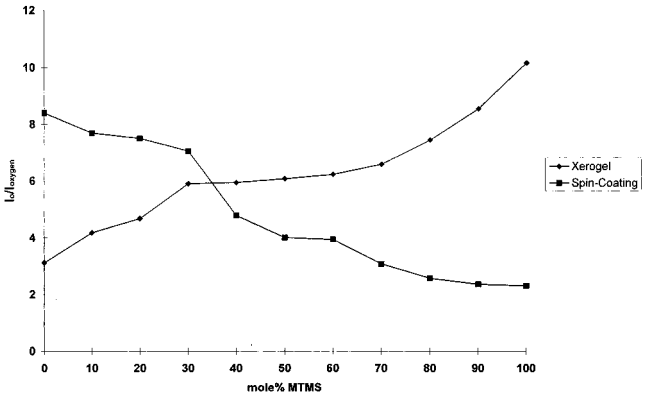

Figure 8. Comparison of Stern−Volmer quenching ratio as a function of mole percent MTMS and gel formation.

network,[35] resulting in the formation of a less compacted thin film by spin-coating. Hence, the less porous, more compact structure of the organically modified spin-coated thin films along with decreased surface $Si-CH_3$ groups in these films (as observed via XPS) causes a lower Stern−Volmer ratio and oxygen sensitivity in Ru(II)-doped ORMOSIL thin film samples.

IV.1.3. Xerogels vs Spin-Coated Thin Films. On the basis of the quenching data, spin-coating MTMS reduces the Stern−Volmer ratio by a factor of 5, whereas spin-coating TEOS raises this ratio by a factor of 2.7. As shown in Figure 8, MTMS additions of greater than 30% double the Stern−Volmer ratio in the xerogels until a plateau is reached at 80% MTMS. On the other hand, MTMS additions of more than 40% in the spin-coated films significantly reduce the Stern−Volmer ratio. Furthermore, spin-coated samples possess a greater contribution from the weaker contributing K_{SV} value (and the short lifetime component) than the xerogels. This result suggests that the spin-coated films contain more heterogeneous sites than the xerogels.

It may be hypothesized that the dynamic removal of solvent upon spinning prevents molecular reorientation upon drying. Thus, Ru(II) molecules do not access their lowest energy state configuration in the films. Consequently, the Ru(II) molecules are "locked-in" to their position upon solvent evaporation.

Conclusions

Luminescence decay analysis of ruthenium(II)−tris-4,7-diphenyl-1,10-phenanthroline dichloride, embedded in organically modified xerogel monoliths, revealed that increased additions of MTMS improved the Stern−Volmer quenching ratio and the sensitivity to low oxygen concentrations. This improved quenching was attributed to the increased oxygen diffusivity in the more hydrophobic MTMS-modified gels. Spin-coated thin films doped with Ru(II) showed contradictory luminescence quenching behavior to that of the bulk gels in that increased MTMS additions provided a decreased Stern−Volmer ratio. XPS and ellipsometric studies indicated that the decreased quenching in the ORMOSIL spin-coated thin films was due to a less porous and less hydrophobic film structure as compared to the bulk ORMOSIL gels. The greater Stern−Volmer ratio in TEOS spin-coated films, doped with the Ru(II) complex, versus the TEOS xerogels was attributed to the higher porosity of the thin film structure. In summary, favorable sol−gel oxygen sensors are derived from MTMS xerogels or TEOS spin-coated films. This conclusion is based upon the improved Stern−Volmer ratios observed in these systems over the films or xerogels of different compositions.

Acknowledgment. The authors would like to acknowledge the generous support for this research provided by the National Science Foundation (NSF), the New Jersey Commission on Science and Technology (NJCST), and the Fiber Optic Materials Research Program (FOMRP) at Rutgers University.

CM9802806